Comparison of Alpha/Beta and high-gamma band for motor-imagery based BCI control: A qualitative study

Conference Paper · October 2017

DOI: 10.1109/SMC.2017.8122965

CITATIONS
3

READS
175

6 authors, including:

Johannes Gruenwald
g.tec
12 PUBLICATIONS **11** CITATIONS
SEE PROFILE

Christoph Kapeller
g.tec
58 PUBLICATIONS **561** CITATIONS
SEE PROFILE

Christoph Guger
g.tec medical engineering GmbH
338 PUBLICATIONS **7,593** CITATIONS
SEE PROFILE

Kyousuke Kamada
Asahikawa Medical University
125 PUBLICATIONS **1,750** CITATIONS
SEE PROFILE

Comparison of Alpha/Beta and High-Gamma Band for Motor-Imagery based BCI Control*

A qualitative Study

J. Gruenwald, C. Kapeller, C. Guger
Research and Development
g.tec medical engineering
Schiedlberg, Austria
gruenwald@gtec.at

H. Ogawa, K. Kamada
Dept. of Neurosurgery
Asahikawa Medical University
Asahikawa, Japan

J. Scharinger
Dept. of Computational Perception
Johannes Kepler University
Linz, Austria

***Abstract*—Brain waves contain manifold information about ongoing cognitive processes and related body function. This information, such as power changes in certain frequency bands, can be extracted and interpreted by brain-computer interfaces (BCI). For this publication, we re-evaluated data from two subjects with implanted subdural electrodes who participated in a two-class BCI motor imagery experiment with online feedback. In particular, we compared classification accuracy based on bandpower features extracted from a low-frequency band (LFB, Alpha/Beta, 8-32 Hz) and a high-frequency band (HFB, High-Gamma, 110-140 Hz). The signal processing chain involved bandpower computation, spatial filtering via Common Spatial Patterns (CSP), computing the log-normalized variance, and finally classifying via Linear Discriminant Analysis (LDA). For comparison, we also re-evaluated a comparable motor execution experiment with the same participants.**

Results of the motor imagery experiments revealed that features derived from the LFB provide consistently higher classification accuracies than features derived from the HFB. In contrast to that, HFB-based features outperform LFB-based features for conventional motor execution experiments.

Keywords—brain-computer interface, motor imagery, alpha band, beta band, high-gamma band, event-related desynchronization, high-gamma activation, common spatial patterns, linear discriminant analysis

I. Introduction

The Brain-Computer Interface (BCI) establishes a communication channel from a person's mind to the environment without physical movement [1], [2]. This requires the electrophysiological acquisition of brain waves, of which the most commonly used techniques are the non-invasive and well-known electroencephalogram (EEG) and the invasive electrocorticogram (ECoG), where electric potentials are directly sensed from the cortex via subdural electrodes. ECoG signals outperform EEG signals in terms of temporal, spectral, and spatial resolution. This superiority of invasive systems, however, is relativized by their limited applicability, i.e., to the clinical context where neurosurgical intervention is an option.

Brain waves and their information content are subject to extensive research. It has been shown that dependent on the experiment, different characteristics can be observed and certain behavior can be provoked. In particular, one important feature exploited by BCIs is the fact that physical movement is related to changes in the power within certain frequency bands of brain waves. In this scenario, bandpower in low-frequency bands (LFB, Alpha and Beta, 8-32 Hz) decreases, whereas bandpower in high-frequency bands (HFB, Gamma and High-Gamma, above 32 Hz) increases. This phenomenon is termed event-related desynchronization (ERD, occurring in the LFB) and broadband or High-Gamma activation (HGA, occurring in the HFB), respectively [3]–[6]. The transients of ERD are much slower, and its spatial distribution on the cortex is comparably smooth. It is believed to reflect processing sensory or cognitive information or preparation of motor movement [3]. HGA, on the other hand, is linked for example to actual motor movement and exhibits much higher temporal and spatial resolution [7]. Changes in the HFB are coupled with the phase of low-frequency rhythms such as Theta- and/or Alpha-oscillations [8], [9]. When it comes to plain imagination of motor movement (also termed motor imagery), it is known that imagination-based ERD is comparable to ERD that stems from actual movement. However, the amplitude of HGA is smaller [10]. This supports the theory that HGA is linked to actual movement, which is not occurring during mere imagination.

Classification of actual and imagined movement is a well-studied field and the underlying principle of many BCI applications [11]–[16]. These systems are usually cue-based, where the subject has to perform or imagine certain types of movement indicated by a visual or auditory stimulus. The data is then collected in trials, which are used to train and test the system.

In this publication, we present the re-evaluation of an ECoG-study conducted with two subjects who participated in motor imagery and motor execution experiments. In particular, we investigated if ERD or HGA provides better bandpower features to improve classification accuracy. Although our analyses were conducted offline and a-posteriori, we used a causal processing pipeline. This allows its usage in future online experiments.

II. Methods

A. Subjects and Setup

We used ECoG data from two patients P1 and P2 who volunteered to participate in this study. They suffer from intractable

This work was supported by the *European Union FP7 Integrated Project VERE* and the *EuroStars RapidMaps 2020* project.

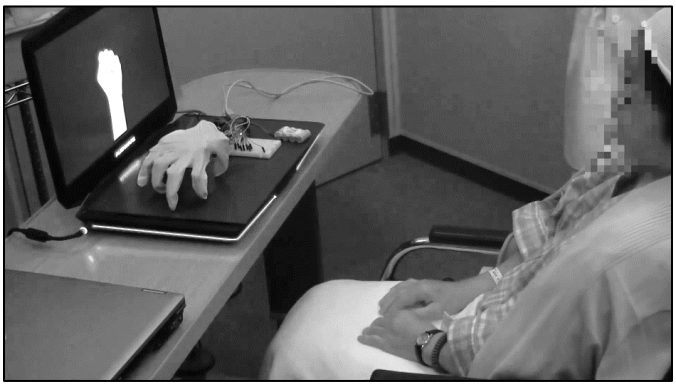

Fig. 1. Motor imagery experiment with online feedback.

epilepsy and underwent neuro-monitoring at Asahikawa Medical University, Japan, in the course of their surgical treatment. Both patients had several subdural electrode grids implanted, but only data from a 60-channel microelectrode array covering the motor cortex was used for signal analysis. The electrode grids were connected to a bio-signal amplifier, which digitized the data at 1200 Hz and provided it to the connected PC. Data processing was carried out in MATLAB (The MathWorks, Inc.).

B. Experiment Protocol

1) Motor Imagery Experiment

Both patients participated in a cue-based motor imagery experiment with online feedback as shown in Fig. 1. In a randomized order, visual stimuli were shown on a screen, indicating that the patient should imagine to make either a fist or stay at rest. Stimulus duration was 3.5 seconds for P1 and 4.0 seconds for P2. The time interval between the stimuli was randomized between 2.15 and 2.65 seconds for P1 and between 2.4 and 3.6 seconds for P2. Feedback was given by a robotic hand which mimicked poses of either an open hand (i.e., rest) or a fist, dependent on a classification result evaluated after each trial. P1 completed 160 trials in 2 runs (80 per class), and P2 completed 296 trials in 8 runs (148 per class).

2) Motor Execution Experiment

Both patients also participated in a cue-based motor execution experiment. Similar as above, a randomized stimulus appeared on the screen, indicating that the patient should either make a fist or to stay at rest[1]. Stimulus duration was set between 1 and 2 seconds for different sessions of the experiment. The time interval between the stimulus onsets varied randomly between 4 and 5 seconds. P1 was also provided with online feedback via a robotic hand as described above, completing 180 trials in 3 runs (90 per class). P2 completed 160 trials in 2 runs (80 per class).

C. Signal Processing

Here, we outline the signal processing framework as presented in Fig. 2. An overview of the processing parameters is given in Table I. The LFB was set to 8-32 Hz according to literature [10]. For the HFB, several options exist. Considering interfering harmonics of the power line at multiples of 50 Hz, we chose 110-140 Hz since preliminary analyses yielded better performance compared to 60-90 Hz, 160-190 Hz, or all bands together. Similarly, the size and relative position of windows were specified to maximize classification accuracy for the respective experiment and frequency band.

[1]Actually, the experiment comprised a third class (making a "Peace" gesture). Since this class does not contribute to our analysis, it was neglected.

TABLE I. PROCESSING PARAMETERS, OVERVIEW

Experiment	Frequency Band	T_{CSP} [a]	T_{var} [b]	T_{LDA} [c]	T_{eval} [d]
Motor Imagery	LFB 8 – 32 Hz	2.0 ... 4.0	1.0	3.0	2.5 ... 3.5
	HFB 110 – 140 Hz	1.0 ... 3.0		2.0	1.5 ... 2.5
Motor Execution	LFB 8 – 32 Hz	1.0 ... 2.0	0.5	1.5	1.25 ... 1.75
	HFB 110 – 140 Hz	1.0 ... 1.3		1.15	1.1 ... 1.2

All values are given in seconds. See text for further description.
[a] CSP evaluation time interval, given relative to cue onset.
[b] Variance window length.
[c] LDA training point in time, given relative to cue onset.
[d] Classifier evaluation window, given relative to cue onset.

1) Preprocessing

In an initial step, the ECoG signals were band-pass filtered according to the frequency band of interest (IIR 5th order Butterworth filter, only forward filtering). For convenience and to decrease processing time, the results were decimated to a sampling rate of 400 Hz. The signal was then triggered, i.e., split into trial segments aligned to the rising edge of a trigger signal and labeled by the respective class.

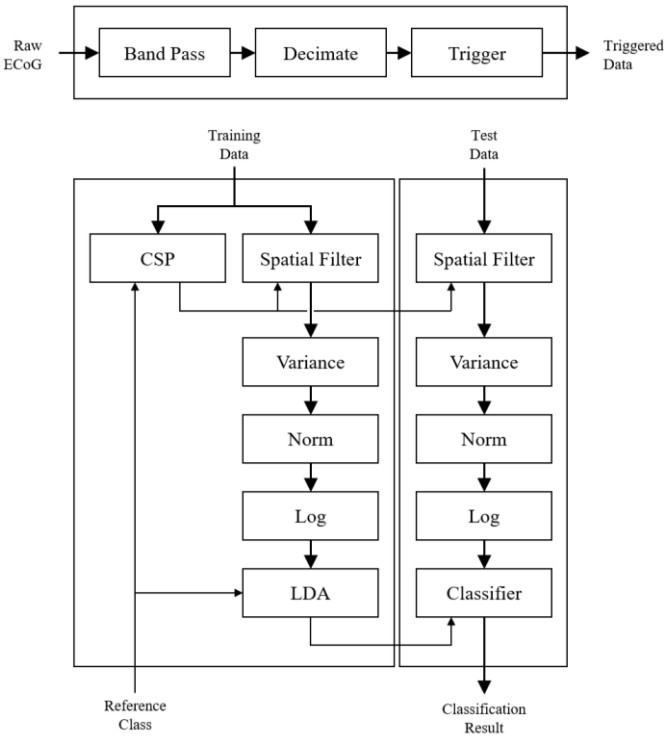

Fig. 2. Signal processing framework.

2) Data Partitioning

We followed the approach of predicting the class label of a trial by a classifier system trained on the 20 preceding trials, where the training was repeated each new trial. To obtain evenly distributed classes in the training set, the (initially randomized) trials were sorted towards alternating class labels, keeping the original order roughly intact.

3) Training

Given triggered and labeled training data as resulting from the preprocessing chain, the respective training set was processed in the following manner: First, Common Spatial Patterns (CSP) [17] were computed to maximize spatial discriminability and to reduce feature dimensionality according to the window T_{CSP} as specified in Table I. After projecting the signal channels onto the four most discriminative CSP vectors, the log-normalized power of the resulting features was obtained as follows: First, the variance in a sliding window of size T_{var} (cf. Table I) was computed. Advancing this window by 10 samples reduced the effective sampling rate further, i.e., from 400 Hz to 40 Hz. The resulting values were then normalized by the total variance over all four feature dimensions. Finally, the logarithm was taken, which has the benefit of yielding distributions with constant variance if taken from power signals [18]. Based on these features, a classifier based on Linear Discriminant Analysis (LDA) was trained at time point T_{LDA}, which was set to the center of the CSP window.

4) Test

For testing, the data were processed identically to the training stage, with the exception that the previously trained CSP and LDA weights were used. Over the time course of each tested trial, one signal segment containing the classification result (and binary accuracy values) was obtained. Fig. 3 shows exemplary grand averages of these signal segments.

III. Results & Discussion

1) Within-Trial Accuracy

To illustrate the different cortical activation transients of the two experiments, Fig. 3 shows two examples of the within-trial classification accuracy, relative to the cue onset and averaged over all test trials.

It can be clearly observed that motor imagery (Fig. 3, left) causes a smooth activation curve. This is plausible since imagination is per se a highly volatile process whose onset and intensity can't be quantified by objective criteria and must be assumed to vary considerably over trials – leading to a smeared temporal average. The sustained activation justifies wide evaluation windows, as indicated by the shaded areas (see figure caption for details). Overall, the superiority of LFB-based classification over HFB-based classification by around 20% is striking. The reason for the comparably and somewhat unexpectedly low accuracy of HFB-based classification may be explained as follows: since HGA is linked to actual motor movement, a smaller amplitude of power changes in the HFB is plausible and can be expected (as already reported [10]). This explains the deterioration of HFB-based classification up to a certain degree. Second, HGA is known to be a spiky signal with pronounced transients compared to ERD [3]. These characteristics of HGA are clearly beneficial for experiments with quantifiable and controllable actions (such as movement) – but at the same time, they are disadvantageous for imagery paradigms that cause temporally diffuse cortical activation.

In contrast to motor imagery, motor execution is a much better defined process in terms of transients and intensity, and identical repetition is easy. This is reflected particularly by the pronounced accuracy curves of HFB-based classification (Fig. 3, right). Its peak activation is of short duration, requiring a small evaluation window. Nonetheless, HFB-based classification yields high accuracy values within this short time frame, surpassing 90%. In contrast to that, LFB-based classification yields a maximum accuracy at around 75%, leaving a headroom of 15% compared to the HFB.

2) Accuracy Trend

Fig. 4 gives a more conclusive picture of the overall performance for both patients and experiments by showing the accuracy trend over time across the whole experiment. To obtain this trend, one single classification result per trial had first to be extracted from the within-trial classification signal segment as resulting from the processing chain (cf. Section II.C.4). To this end, for each trial segment all classification results within a fixed window T_{eval} (cf. Table I and illustration in Fig. 3) were evaluated. As overall classification result of the respective trial, the

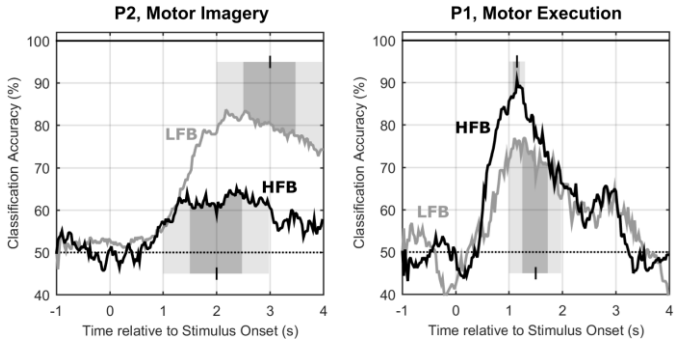

Fig. 3. Classification accuracy over time, relative to stimulus onset and averaged over all test trials. The shaded areas indicate (light) the CSP windows T_{CSP} (cf. Section II.C.3) and Table I), and (dark) the classifier evaluation window T_{eval} (cf. Section III.2). The vertical strokes refer to the point in time at which the LDA classifier was trained (T_{LDA}, cf. Section II.C.3) and Table I).

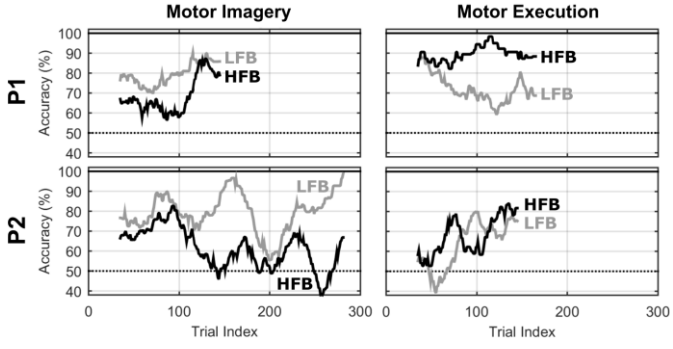

Fig. 4. Accuracy trend over time (i.e., binary accuracy values, smoothed by a 30-tap moving average filter). Note that the trend curves are centered about the moving-average window, such that they start at index 35 (20 initial training samples plus 15 samples referring to half the windows size) and end 15 samples before the overall trial count of the respective experiment.

class who got the most votes within this window was chosen. Consequently, one binary accuracy value per trial was obtained. These values were then processed by a 30-tap moving average filter, yielding the accuracy trend as shown in Fig. 4.

For the motor imagery experiment, it is interesting that over all trials, classification accuracy based on features from the LFB is systematically superior to that based on the HFB (Fig. 4, left column). This was already anticipated in the previous section and Fig. 3 (left). It is yet remarkable how systematic over time this advantage is. Beyond that, LFB-based classification of motor imagery tasks appears to achieve even better performance than LFB-based classification of actual motor execution tasks (comparing left and right column of Fig. 4). This is interesting since one might assume that the planning phases are somewhat similar for both tasks. However, it may be explained by the longer stimulus duration of 3.5 to 4 seconds during the motor imagery experiment (compared to 1 to 2 seconds during the motor execution experiment), which may have led to a more sustaining and discriminative ERD.

For the motor execution experiment, HFB-based classification clearly outperforms LFB-based classification – especially for P1 (Fig. 4, top right; also Fig. 3, right). When reviewing measurement notes and video footage of the motor execution experiment of P2, we noticed that the patients had severe difficulties accomplishing trials 60 to 120 due to lack of concentration. This is evidenced by the respective performance drop visible in Fig. 4, bottom right. It may be interesting to investigate the fact why this issue only affected the HFB but not the LFB, however, it does not contradict the message that for motor execution paradigms, the HFB should be chosen for classification.

IV. Conclusions

In this study, we investigated the quality of bandpower features for brain-computer interfaces (BCI) in terms of classification accuracy of binary motor imagery experiments and related the results to motor execution experiments. In this context, we compared features based on event-related desynchronization (ERD) in a low-frequency band (LFB, 8-32 Hz) to features based on High-Gamma activation (HGA) in a high-frequency band (HFB, 110-140 Hz). We evaluated data from two patients with implanted subdural electrodes, who participated in the experiments during neuro-monitoring in the course of epilepsy treatment.

For motor imagery experiments, our results give clear evidence that bandpower features from the LFB yield a systematically higher classification accuracy than bandpower features extracted from the HFB. This is in contrast to motor execution experiments, where the opposite is true.

Future work may focus on a deeper analysis of the issue why LFB-based classification appears to perform better in motor imagery experiments than in motor execution experiments.

References

[1] J. R. Wolpaw, N. Birbaumer, D. J. McFarland, G. Pfurtscheller, and T. M. Vaughan, "Brain–computer interfaces for communication and control," *Clin. Neurophysiol.*, vol. 113, no. 6, pp. 767–791, Jun. 2002.

[2] J. R. Wolpaw and E. W. Wolpaw, *Brain-Computer Interfaces: Principles and Practice*, 1st ed. Oxford ; New York: Oxford Univ Pr, 2012.

[3] G. Pfurtscheller and F. L. Da Silva, "Event-related EEG/MEG synchronization and desynchronization: basic principles," *Clin. Neurophysiol.*, vol. 110, no. 11, pp. 1842–1857, 1999.

[4] N. E. Crone *et al.*, "Functional mapping of human sensorimotor cortex with electrocorticographic spectral analysis," *Brain*, vol. 121, no. Pt 12, pp. 2271–2299, 1998.

[5] J. R. Manning, J. Jacobs, I. Fried, and M. J. Kahana, "Broadband Shifts in Local Field Potential Power Spectra Are Correlated with Single-Neuron Spiking in Humans," *J. Neurosci.*, vol. 29, no. 43, pp. 13613–13620, Oct. 2009.

[6] K. J. Miller, C. J. Honey, D. Hermes, R. P. Rao, M. denNijs, and J. G. Ojemann, "Broadband changes in the cortical surface potential track activation of functionally diverse neuronal populations," *NeuroImage*, vol. 85, pp. 711–720, Jan. 2014.

[7] K. J. Miller *et al.*, "Spectral Changes in Cortical Surface Potentials during Motor Movement," *J. Neurosci.*, vol. 27, no. 9, pp. 2424–2432, Feb. 2007.

[8] R. T. Canolty and R. T. Knight, "The functional role of cross-frequency coupling," *Trends Cogn. Sci.*, vol. 14, no. 11, pp. 506–515, Nov. 2010.

[9] B. Voytek, R. T. Canolty, A. Shestyuk, N. E. Crone, J. Parvizi, and R. T. Knight, "Shifts in Gamma Phase–Amplitude Coupling Frequency from Theta to Alpha Over Posterior Cortex During Visual Tasks," *Front. Hum. Neurosci.*, vol. 4, Oct. 2010.

[10] K. J. Miller, G. Schalk, E. E. Fetz, M. den Nijs, J. G. Ojemann, and R. P. N. Rao, "Cortical activity during motor execution, motor imagery, and imagery-based online feedback," *Proc. Natl. Acad. Sci.*, vol. 107, no. 9, pp. 4430–4435, Mar. 2010.

[11] J. R. Wolpaw, D. J. McFarland, G. W. Neat, and C. A. Forneris, "An EEG-based brain-computer interface for cursor control," *Electroencephalogr. Clin. Neurophysiol.*, vol. 78, no. 3, pp. 252–259, Mar. 1991.

[12] L. R. Hochberg *et al.*, "Reach and grasp by people with tetraplegia using a neurally controlled robotic arm," *Nature*, vol. 485, no. 7398, pp. 372–375, May 2012.

[13] G. Hotson *et al.*, "Individual finger control of a modular prosthetic limb using high-density electrocorticography in a human subject," *J. Neural Eng.*, vol. 13, no. 2, p. 026017, 2016.

[14] N. Sharma *et al.*, "Motor Imagery After Subcortical Stroke: A Functional Magnetic Resonance Imaging Study," *Stroke*, vol. 40, no. 4, pp. 1315–1324, Apr. 2009.

[15] C. Chatelle, S. Chennu, Q. Noirhomme, D. Cruse, A. M. Owen, and S. Laureys, "Brain-computer interfacing in disorders of consciousness," *Brain Inj.*, vol. 26, no. 12, pp. 1510–1522, 2012.

[16] C. Guger, G. Edlinger, W. Harkam, I. Niedermayer, and G. Pfurtscheller, "How many people are able to operate an EEG-based brain-computer interface (BCI)?," *Neural Syst. Rehabil. Eng. IEEE Trans. On*, vol. 11, no. 2, pp. 145–147, 2003.

[17] J. Müller-Gerking, G. Pfurtscheller, and H. Flyvbjerg, "Designing optimal spatial filters for single-trial EEG classification in a movement task," *Clin. Neurophysiol.*, vol. 110, no. 5, pp. 787–798, 1999.

[18] M. S. Bartlett and D. G. Kendall, "The Statistical Analysis of Variance-Heterogeneity and the Logarithmic Transformation," *Suppl. J. R. Stat. Soc.*, vol. 8, no. 1, pp. 128–138, 1946.